Field Measurements of Wind Loads on Heliostats in an Operational CSP Tower Plant

Matthew Emes, Ulrike Egerer, Scott Dana, Shashank Yellapantula, Mark Mehos, Guangdong Zhu

SolarPACES Conference

September 25, 2025

Photo by Josh Bauer / Bryan Bechtold, NREL 82067

This presentation was produced when the laboratory operated as the National Renewable Energy Laboratory (NREL). The laboratory is now the National Laboratory of the Rockies (NLR).

Contents

1 Introduction

2 Objectives

3 Wind and Loads Instrumentation

4 Case Study 1 – Northerly High Wind

5 Case Study 2 – Southerly High Wind

6 Key Insights and Takeaways

7 Conclusions and Next Steps

Introduction

- Limited data and published literature on wind-induced loads and deformations of heliostats in operational CSP power tower plants
- Such data is necessary to quantify wind effects on tracking deviations and spillage losses in heliostat field cost/performance assessment of CSP plants

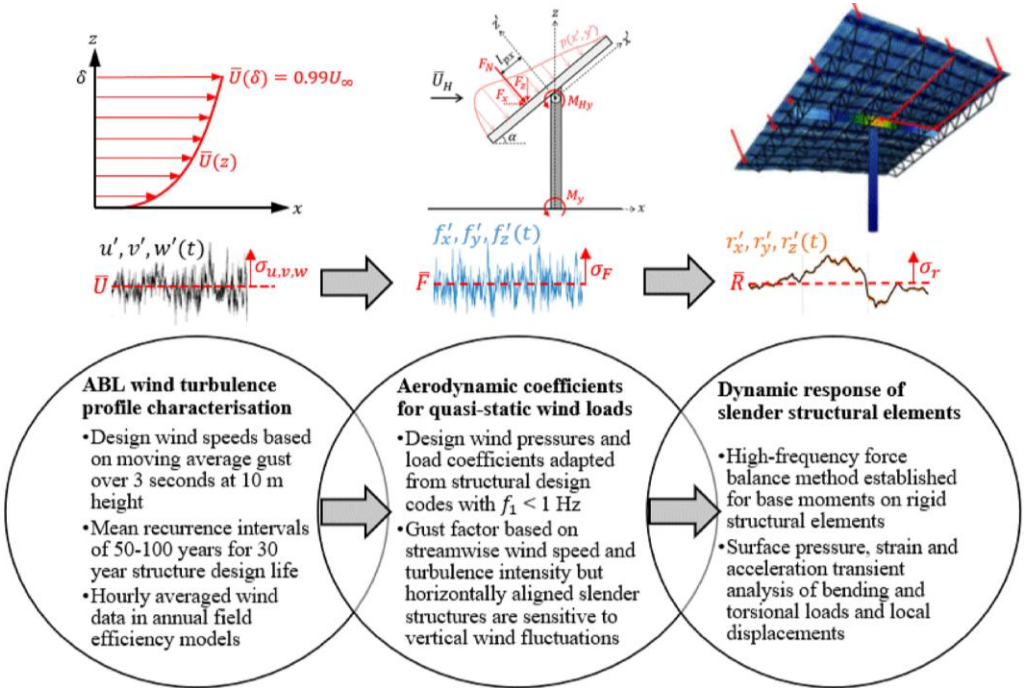

*Emes et al. (2024). "Heliostat Consortium: Gap Analysis on State of the Art in Wind Load Design." Journal of Solar Energy Engineering, Volume 146 (Issue 6): Page 061001.*https://doi.org/10.1115/1.4065429.

Objectives

- In-situ collection of wind and loads on 3 heliostats in an operational power tower plant
- Characterize the effects of localized wind speed, wind direction and atmospheric turbulence on heliostat loading
- Compare and verify non-dimensional load coefficients with scale model heliostats in wind tunnel experiments

Wind and Loads Instrumentation at Operational Heliostat Field

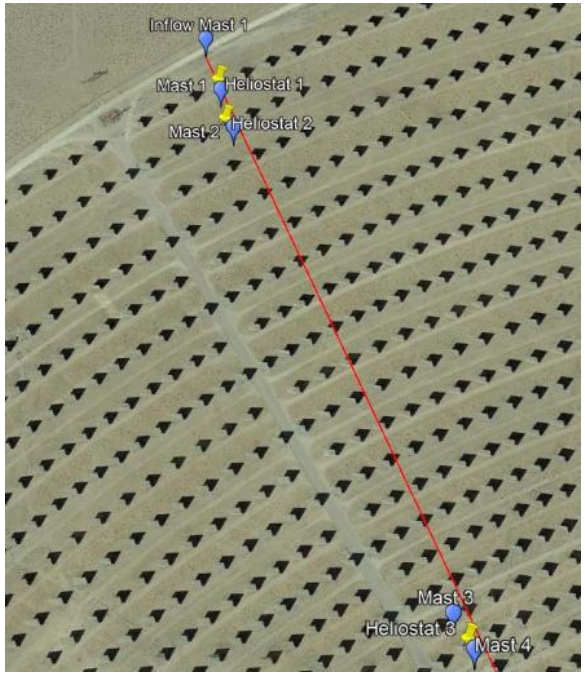

Image from Google Earth

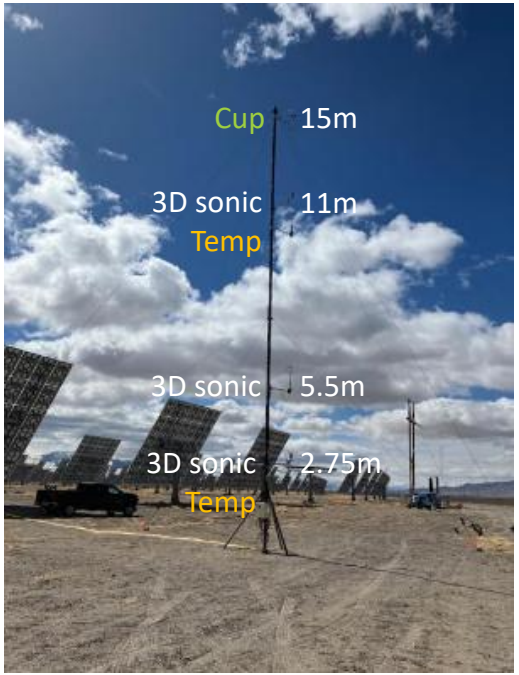

Photo by David Jager, NREL

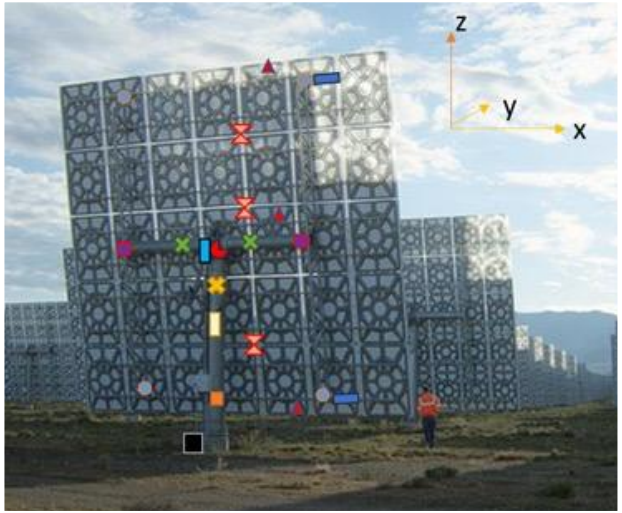

Photo by Scott Dana, NREL

- Pedestal bending strain gage
- Torque tube torque strain gage
- Pedestal torque strain gage
- Pedestal axial strain gage for lift forces
- Accelerometers on facet support structure
- Mirror facet laser displacement sensor
- Dynamic tilt inclinometer
- Support frame bending strain gage
- Differential pressure sensor between facets

Case Study 1 – Northerly High Wind

- Reduced localized wind velocity and increased TKE in interior of the field during operation
- H3 stowed 30 mins before H1 and H2

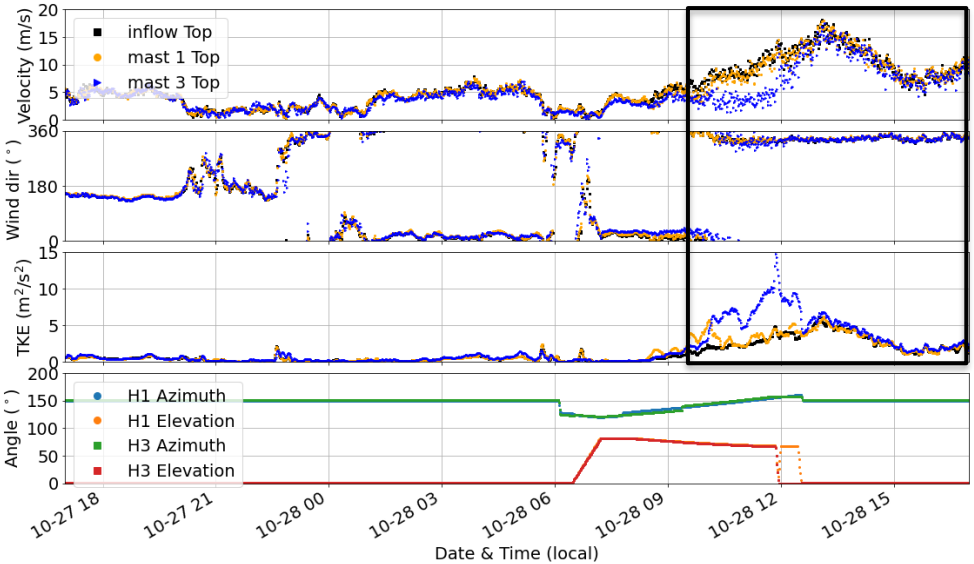

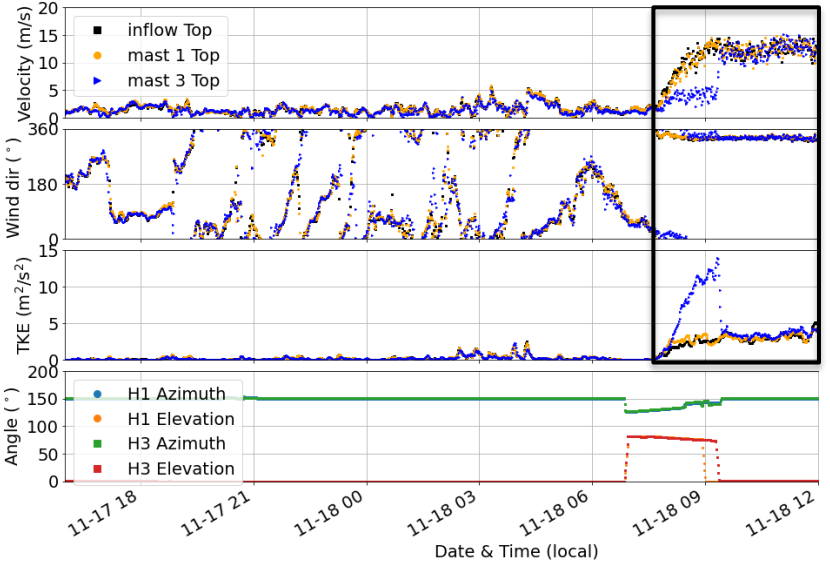

- Shielding of downstream rows with increased turbulence and ~50% decrease in mean velocity at H3 compared to H1
- H1 and H2 stowed 30 mins before H3

Case Study 2 – Southerly High Wind

- Reduced wind velocity and increased TKE and TI in interior of the field during operation (same as northerly wind)
- Small variations in wind and turbulence between interior (mast 3) and field edge (mast 1 and inflow) in stow

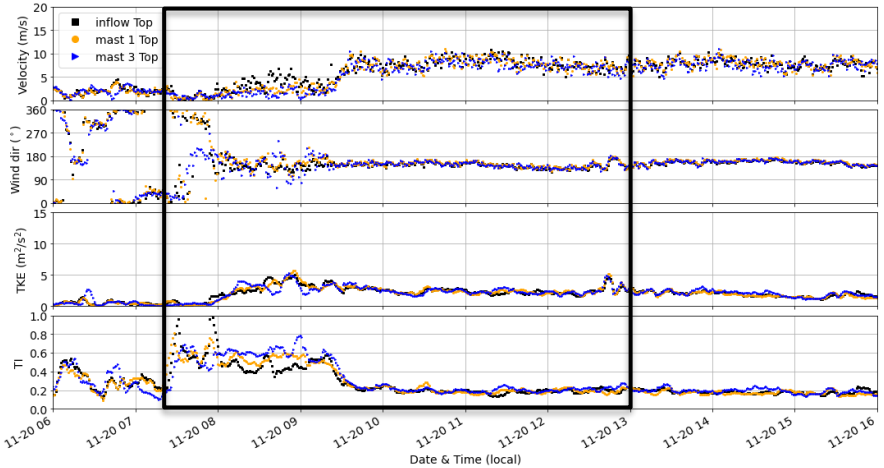

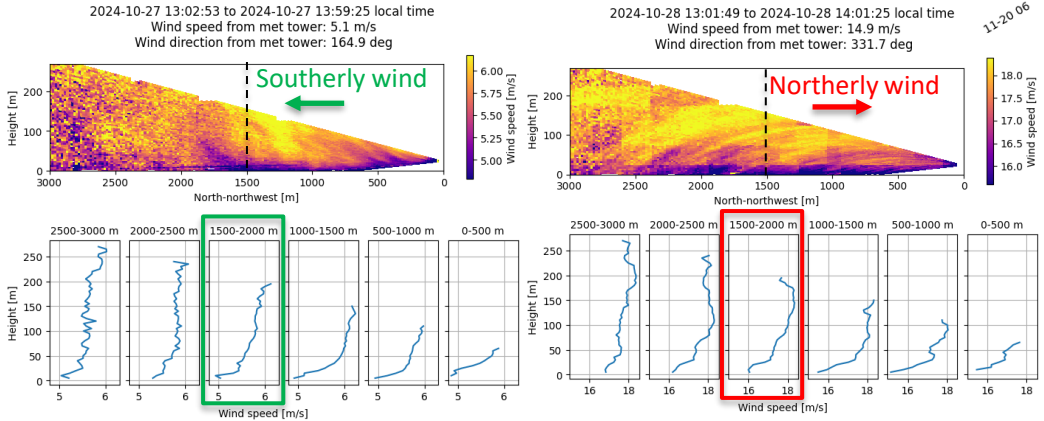

- Scanning LIDAR on heater bay of plant pointing to north-western quadrant of field
- LIDAR mean velocity at 10 m height within 4.3% (southerly) and 6.6% (northerly) of sonic mean at 11m on inflow met tower

Differential Pressure Sensors ΔP

$$F_N = \Delta P_1 A_1 + \Delta P_2 A_2 + \Delta P_3 A_3$$

$$F_x = F_N \sin\alpha$$

$$F_z = F_N \cos\alpha$$

$$M_{Hy} = \Delta P_3 A_3 x_3 + \Delta P_2 A_2 x_2 - \Delta P_1 A_1 x_1$$

$$C_{Fx} = F_x/(0.5\rho U^2 A)$$
$$C_{Fz} = F_z/(0.5\rho U^2 A)$$
$$C_{MHy} = M_{Hy}/(0.5\rho U^2 Ac)$$

A3=10.3×3.369=34.7m^2
A2=10.3×3.369=34.7m^2
A1=10.3×4.492=46.2676m^2

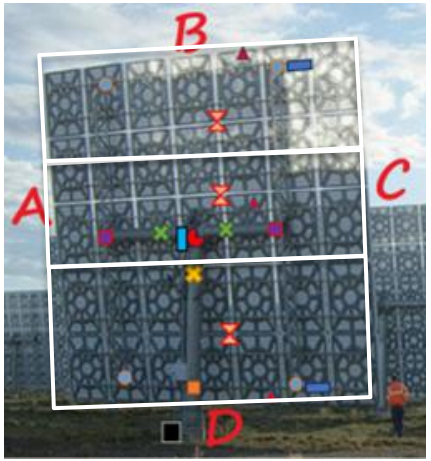

Photos by Scott Dana, NREL

Comparison of Lift Forces from Pedestal Strain Gage and ΔP

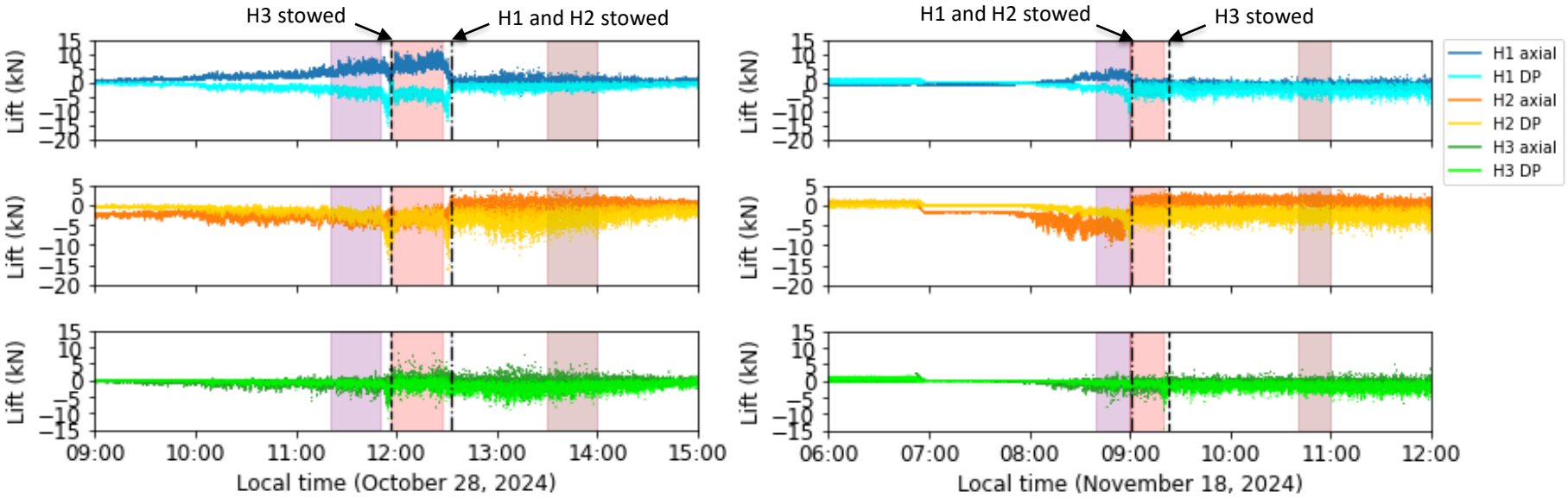

- Good agreement in magnitudes of lift forces calculated from DP sensors with pedestal axial strain gauges on 3 heliostats (H1, H2, H3)
- Load distributions analyzed during three highlighted periods (operating, partial stow, stow)

Lift Force Coefficient Distributions – Northerly Wind

- Non-Gaussian (lognormal) peak distributions for H3 in operation and all 3 heliostats in stow

Peak lift force coefficients (October 28)	Operation (11:20-11:50)			Stow (13:30-14:00)		
	H1	H2	H3	H1	H2	H3
Gaussian (μ + 3σ)	2.19	-2.04	-1.03	0.32	0.35	-0.57
Lognormal (99th percentile)	2.23	-2.08	-1.73	0.74	0.79	-1.22
% difference	2	2	68	131	126	114

Peak lift force coefficients (November 18)	Operation (8:40-9:00)			Stow (10:40-11:00)		
	H1	H2	H3	H1	H2	H3
Gaussian (μ + 3σ)	1.06	-2.65	-0.78	-0.39	0.46	-0.46
Lognormal (99th percentile)	1.15	-2.91	-1.78	-0.89	0.87	-1
% difference	8	10	128	128	89	117

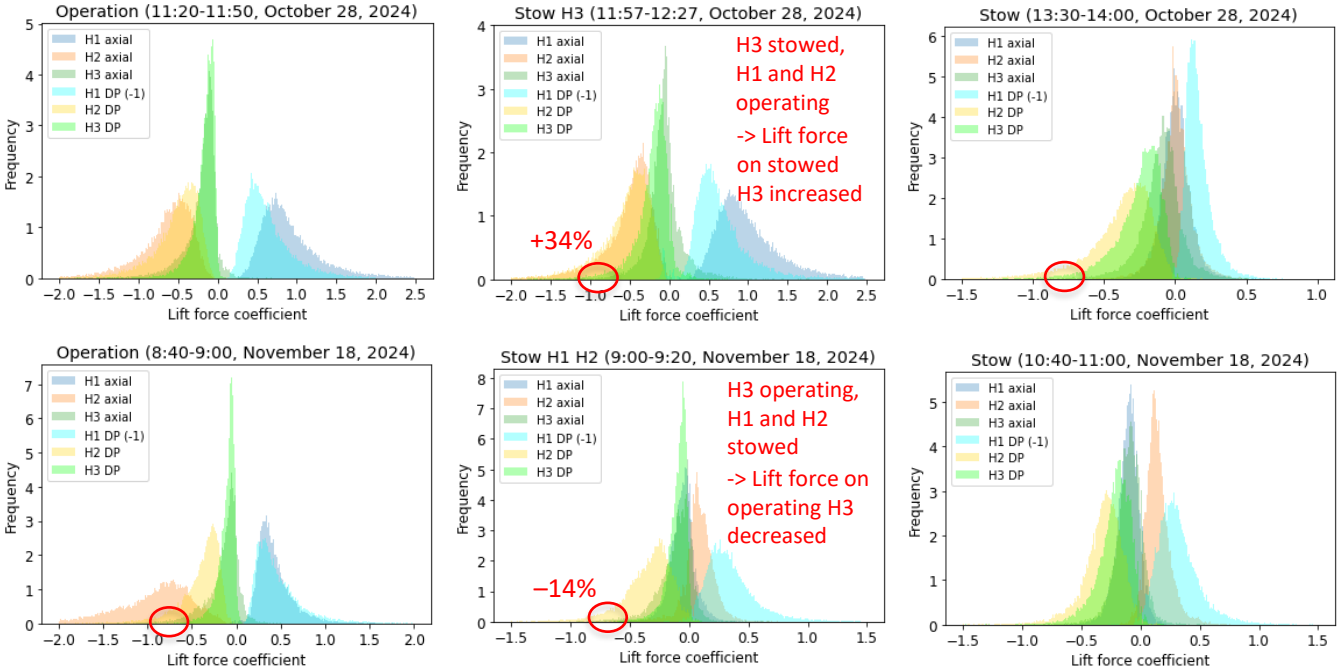

- Orientation of upstream heliostats impacts interior loads
- Stowing upwind field rows first is best practice to reduce interior loads

Lift Force Coefficients – Northerly Wind at CD vs ABLRF vs WT

- Mean and peak operating lift coefficients at 60° elevation at CD within 10% of ABLRF data
- Lift coefficients in stow at 0° elevation with Gaussian peak at CD consistent with WT and lognormal peak at CD consistent with ABLRF

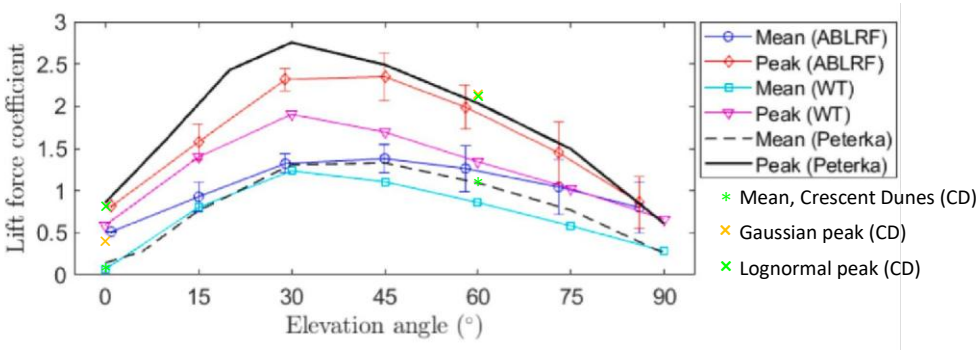

Adapted from Emes *et al.* (2024), *Solar Energy*, https://doi.org/10.1016/j.solener.2024.112742

Source	z_0 (m)	U (m/s)	Iu	Iw	Lux/c	Lwx/c
ABLRF	0.03	6.0	0.25	0.11	27.3	1.56
ESDU 85020	0.03	13.7	0.23	0.12	5.3	0.44
ESDU 85020	0.01	14.7	0.18	0.10	9.8	0.81
ESDU 74031	0.1	12.0	0.30	0.14	15.2	0.10
WT UoA	0.01	6.8	0.12	0.10	1.3	0.53

Lift Force Coefficients Time Series – Northerly and Southerly Wind

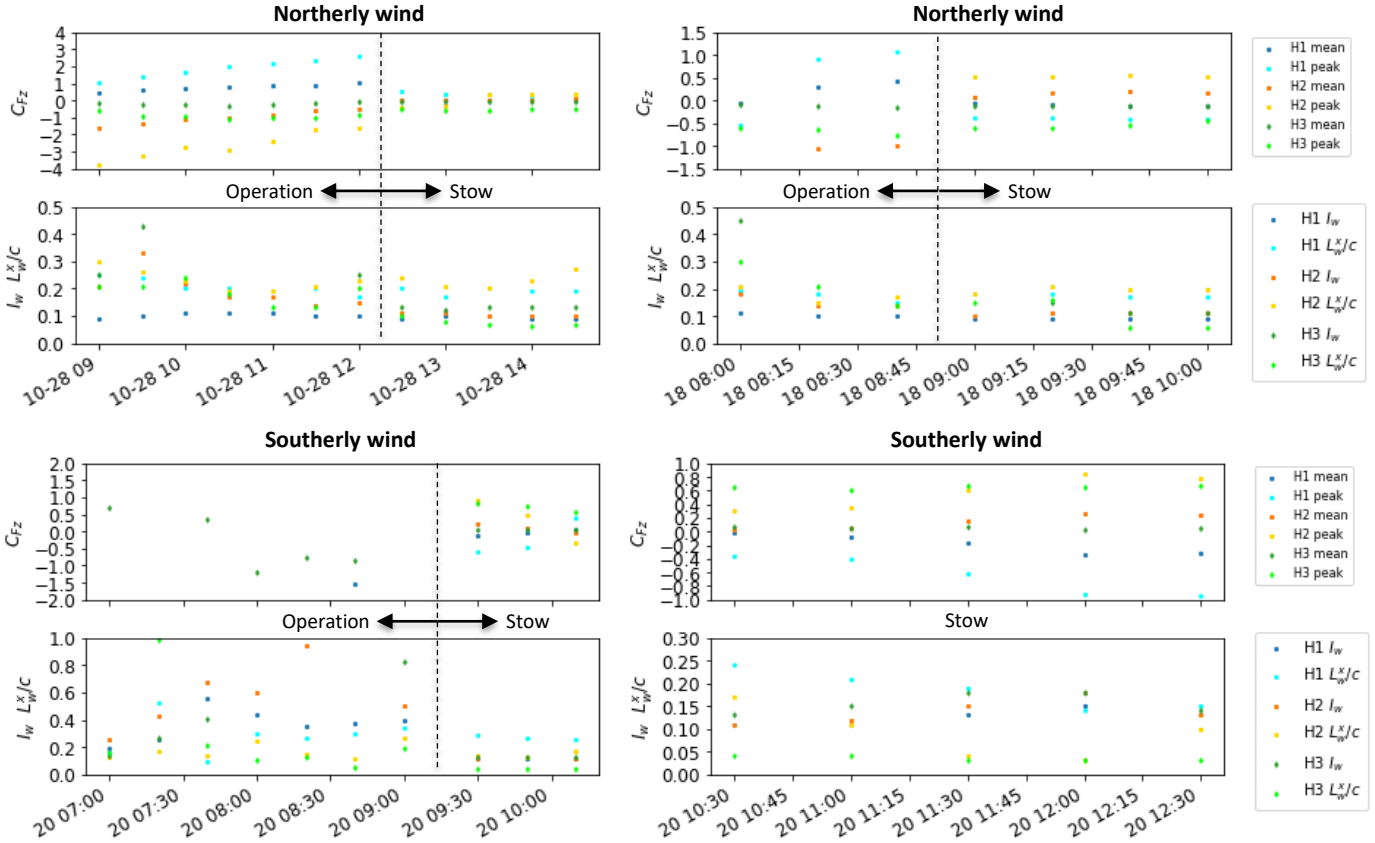

Lift Force Coefficients vs Turbulence – Northerly and Southerly Wind

- Peak lift coefficients increase in the interior (H3) compared to the perimeter (H1, H2) due to increased I_w
- Peak lift and hinge moment coefficients show weak positive linear correlations with I_w and weak negative polynomial correlations with L_w^x/c

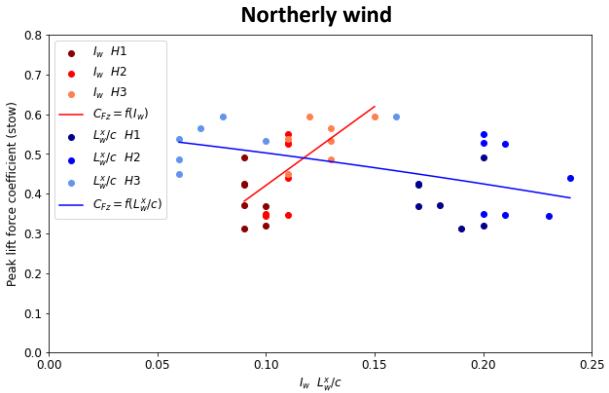

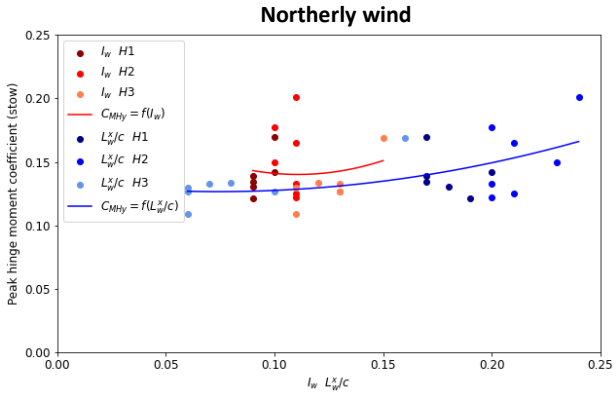

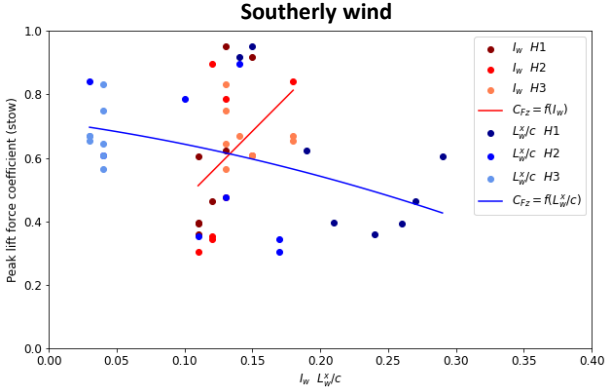

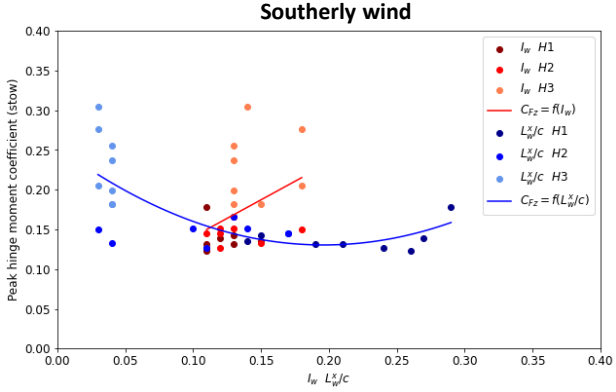

Laser Displacement Sensors on Top and Bottom Mirror Facet Supports

- Two laser displacement sensors mounted on top and bottom facet support beams
- Pointing to back of facet surface (second from western edge)
- Low-wind offsets removed and compensated for temperature

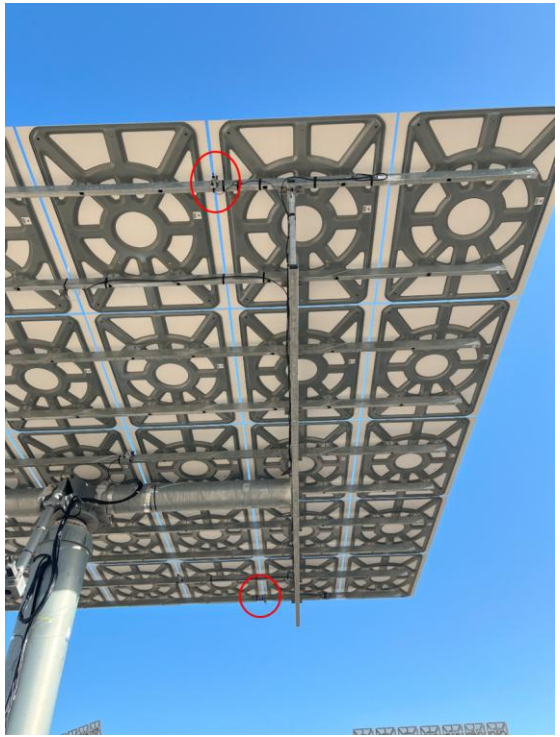

Photos by Scott Dana, NREL

Wind-Induced Facet Displacements

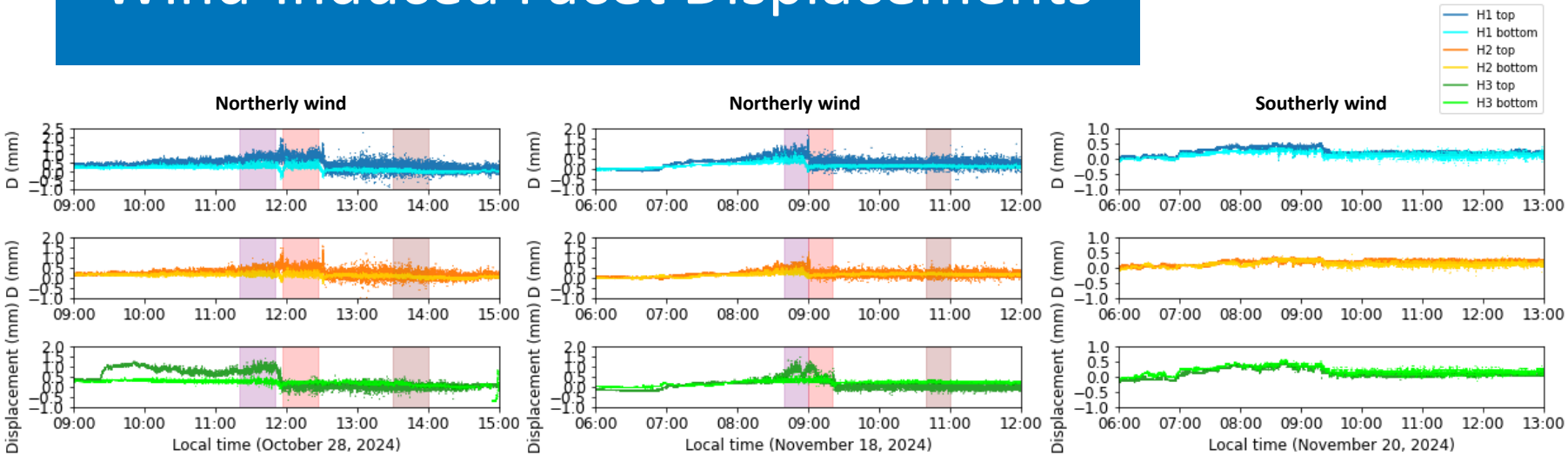

Total reflective surface width $b_s = 10.3$ m
Total reflective surface chord length $c_s = 11.23$ m
Torque tube length $L_{tt} \approx 6$ m

Facet width $b_f \approx b_s/7 = 1.47$ m
Facet height $c_f \approx c_s/5 = 2.25$ m

- For measured out-of-plane facet displacement $r_{z,f} = 2$ mm and small angle approximation

  $\delta_{z,bf} = 2r_{z,f}/b_f =$ **2.7 mrad** $\quad \delta_{z,cf} = 2r_{z,f}/c_f =$ **1.8 mrad**

- For assumed out-of-plane surface displacement $r_{z,s} = 10$ mm* and small angle approximation

  $\delta_{z,bs} = 2r_{z,s}/b =$ **2 mrad** $\quad \delta_{z,cs} = 2r_{z,s}/c =$ **1.8 mrad** $\quad \delta_{z,tt} = 2r_{z,s}/L_{tt} =$ **3.3 mrad**

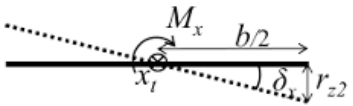

Vasquez Arango *et al.* (2017), Dynamic wind loads on heliostats, RWTH-2016-12225, DLR.

*Blum, Helmer and Pfahl (2024), Dynamic Wind Loading of Heliostats - Efficient Simulation of Resonance Effects, SolarPACES 2024

Key Insights and Takeaways

- Peak **lift coefficients** increase in the interior compared to the field edge for northerly and southerly winds and are correlated to vertical turbulence intensity I_w
- Peak **hinge moment coefficients** increase/decrease in the interior compared to the field edge for southerly/northerly winds and are correlated to vertical turbulence length scale L_w^x/c
- **Interior loads** are strongly dependent on tilt angle of upstream collectors
- Wind tunnel measurements generally a good approximation for mean loads at perimeter but can **underpredict peak load coefficients at stow and small elevation angles in the interior of the field**

Conclusions and Next Steps

- First-of-a-kind dataset reveals insights into localized wind turbulence and dynamic loading at perimeter and interior of an operational heliostat field
- Field measurements show increased unsteady wind and dynamic loads in the field interior in stow position
- Best practice to stow at the upwind field edge before the interior
- Measured facet displacements show significant influence of wind

- Analysis of pedestal torque for azimuth moments and pedestal bending for overturning moment comparison with wind tunnel experiments
- Analysis of wind-induced tracking deviations and accelerations and investigate amplitudes and frequencies of maximum load cases

Thank You

www.nlr.gov

matthew.emes@nlr.gov

NLR/PR-5000-93875

This work was authored by NREL for the U.S. Department of Energy (DOE), operated under Contract No. DE-AC36-08GO28308. Funding provided by U.S. Department of Energy Office of Energy Efficiency and Renewable Energy Solar Energy Technologies Office. The views expressed in the article do not necessarily represent the views of the DOE or the U.S. Government. The U.S. Government retains and the publisher, by accepting the article for publication, acknowledges that the U.S. Government retains a nonexclusive, paid-up, irrevocable, worldwide license to publish or reproduce the published form of this work, or allow others to do so, for U.S. Government purposes.

Photo from Getty-181828180

NREL